Design of an electric Series Elastic Actuated Joint for robotic gait rehabilitation training

Claude Lagoda, *Member, IEEE*, Alfred C. Schouten,
Arno H. A. Stienen, *Member, IEEE*, Edsko E. G. Hekman, Herman van der Kooij

Abstract—Robotic gait rehabilitation is at least as effective as conventional gait training in stroke survivors. Patients must be assisted as needed in order to improve affected gait patterns. The combination of impedance control and series elastic actuation is a viable actuation principle to be used for human robot interaction. Here, a new promising electric series elastic actuated joint is developed. The large torque bandwidth limit at 100 Nm is 6.9 Hz. With a total weight of 3.175 kg it is possible to directly mount the actuator on the exoskeleton frame. The actuator is capable of providing sufficient torque at normal walking speed. Full patient assistance during gait and free motions without impeding the gait pattern are possible. The actuator allows isometric measurements up to 100 Nm and the patient's progress in robotic rehabilitation can be evaluated.

Index Terms—Backdrivability; Impedance control; Rehabilitation; Series Elastic Actuator; Stroke

I. INTRODUCTION

IN present times, health threatening incidences like stroke are on the increase. Stroke, also known as cerebrovascular accident (CVA), is a sudden stop of blood flow to the brain. There are two basic types of stroke: the ischemic stroke where blood supply is interrupted, e.g. blood clots blocking vessels, and the hemorrhagic stroke where a blood vessel breaks and bleeds into the brain. Hence the brain regions located behind the affected vessels are not supplied with blood which causes cell death. The consequences of a stroke, beside of death, range from loss of functions over cognitive symptoms to motor control problems. In most cases this might be temporarily but for some patients the implications last lifelong. Rehabilitation therapy is given to partly restore function and to improve mobility.

There is simultaneously an upward trend for CVA inci-

dences and a decrease in CVA mortality. WHO estimates that 15 million people over the world suffer from stroke each year [1]. Typically in high income countries the mortality rate of stroke victims is decreasing, whereas in low and middle income countries the stroke mortality rate is increasing [10]. It is legitimate to claim that an increase of stroke survivors is induced due to the decrease of mortality in western civilization caused by stroke. Worldwide 5 million stroke survivors remained permanently disabled and require successive health treatments over years [2].

In case of motor control problems, e.g. asymmetrical gait pattern or Hemiplegia, rehabilitation is necessary. Rehabilitation not only improves autonomy, which is an important quality of life, but amongst other also improves the condition of the cardiovascular system, maintains muscle strength and prevents bone deterioration induced by a lack of motor activity. Gait rehabilitation therefore is vital for patients with motor control problems in lower extremities.

Successful gait rehabilitation appears to be due to bihemispheric plasticity of the brain. Cortical reorganization involves recovery of motor control functions. Rehabilitation procedures take advantage of the learning-dependent neuroplasticity and new therapies are being developed [9].

Regarding clinical research, robotic rehabilitation not only allows for new therapy strategies. It can also serve as an assessment tool for a variety of gait related parameters, e.g. torque or speed at joints, and provides information about the success of therapy. It has been shown that robotic rehabilitation is at least as effective as conventional rehabilitation procedures [13].

Assisting the patient as needed is amongst others the most prominent aspect to make robotic rehabilitation successful [4]. It is important to simultaneously activate efferent motor pathways and afferent sensory pathways. Imposing fixed repetitive gait trajectories on limbs causes the motor cortex to habituate to repetitive activation of the same sensory pathways and does not improve gait pattern [6]. Instead, the patient has to be active in this process [11]. With force-field control the patient's leg is assisted as needed to keep the leg on its trajectory [15]. At the moment there are different strategies to create a natural but still personal trajectory for each patient. The benefits of the trajectory creation strategies still have to be clinically proven.

In the Netherlands at the University of Twente a new promising gait rehabilitation trainer, the "LOwer extremity Powered ExoSkeleton" (LOPES) [19], is being developed.
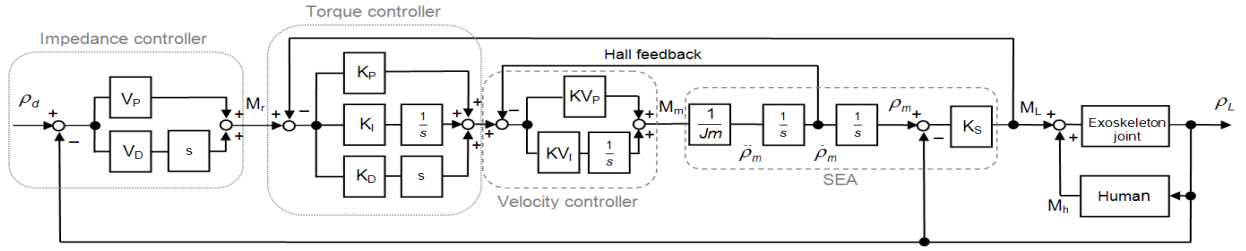
Fig. 1. Control scheme. Impedance is PD controlled and the torque controller is implemented as PID-controller. The velocity controller uses a PI controller with hall sensor feedback from the motor. K_P, V_P, KV_P = proportional gain. K_D, V_D = damping gain. K_I, KV_I = integrative gain. ρ = current position, M = current torque. Indexes: d = desired value, r = reference value for a controller, m = brushless motor, L = load side of SEA and h = generated by the human.

LOPES is referred to as an "interactive neuro-rehabilitation robot" [19] as it implements most strategies for successful rehabilitation and is designed for assist-as-needed (AAN) training. In order to use AAN paradigms the exoskeleton is optimized regarding mechanical structure and actuation principles. Concerning control, assist-as-needed human-robot interaction can be realized with impedance control [7] [8].

LOPES uses series elastic actuation for the actuated joints. A series elastic actuator (SEA) is a drive system in series with a compliant element. Dynamic effects of existing backlash in the gearbox, cogging torque in the motor and friction are largely reduced at the output of the spring. The elastic element serves as an accurate torque source and as a low cost torque sensor. The elastic element also serves as a compliant interface between the human and the robot, protecting the user and drive train from sudden shocks, and improving backdrivability characteristics. A drawback is the reduced large torque bandwidth due to motor saturation [14].

In LOPES the drive system, mounted on an external frame, is connected via Bowden cables to the elastic element, mounted on the exoskeleton segments. It has been found that the Bowden cables are unreliable and fail. It has been decided to develop a new lightweight direct-mounted SEA which can provide sufficient output torque, acceleration and speed to assist the leg of a patient [3] [16] [19].

II. METHODS

A. Requirements

As AAN implies interaction between the human and robot, the control must be inherently safe. LOPES offers different control modes for rehabilitation, i.e. the so-called "robot-in-charge" mode and the "patient-in-charge" mode [19]. Most often the robot will toggle between both modes. These modes are realized with impedance control [7].

Impedance can be described as the relation between actual trajectory position and actuator output force. Deviations from the actual trajectory position result in corrective forces. The magnitude of the force depends on the preset impedance and the extent of trajectory deviation [8].

Looking at the control scheme, see Fig. 1, the impedance controller operates as the higher level controller which tries to control the impedance of the actuator by measuring the actuator's output position and generating an output torque. The lower level controller, the torque controller, monitors and regulates the output torque. Thus the quality of the impedance controller largely depends on the accuracy of the position sensor, and the bandwidth and accuracy of the torque source.

With a SEA the output torque is easily regulated by quantifying the elastic element's deformation with position sensors. The joint position is also quantified by position sensors. This reduces the need for different sensors and makes the control of the actuator more robust [3].

During rehabilitation the exoskeleton frame is connected directly to the leg. Hence, the exoskeleton frame must be as lightweight as possible. Low exoskeleton mass is important as inertia cannot easily be compensated during training. The patient can feel additional inertia which influences the gait pattern. In addition low intrinsic friction on the exoskeleton joints helps increasing actuation bandwidth.

The actuation power and torque demands have been calculated using anthropometric data of the Dutch population [5] and gait data from D. A. Winter [20]. Fig. 2 shows the power and torque demands of the SEA for a 2.088 m tall patient with a weight of 120 kg and 7 kg of exoskeleton mass added to the limb.

The estimated peak torque for the "robot in charge" mode is 76 Nm for the hip and 74 Nm for the knee flexion / extension. Switching from the "patient-in-charge" mode at zero-impedance to the "robot-in-charge" mode with maximal assistance during gait requires more torque. In a worst case scenario the resulting angular output speed will be 9.2 rad/s requiring around 120 Nm. It has been decided to limit the output torque to 100 Nm due to design limitations. See Table 1 for actuator requirements.

Spring stiffness is of essential importance as the elastic element imparts the output torque to the user. The spring stiffness of the existing LOPES design is 353 Nm/rad. This value will be used for the new SEA as the spring stiffness has been found to be a good trade-off between available output torque, actuator bandwidth and human interfacing comfort. The compliant element makes a blocked drive train output backdrivable, but only in a limited way.

LOPES is also used as a measuring tool to collect clinical data which allows for isometric muscle contraction tests, giving more insight into the patient's physical capabilities.
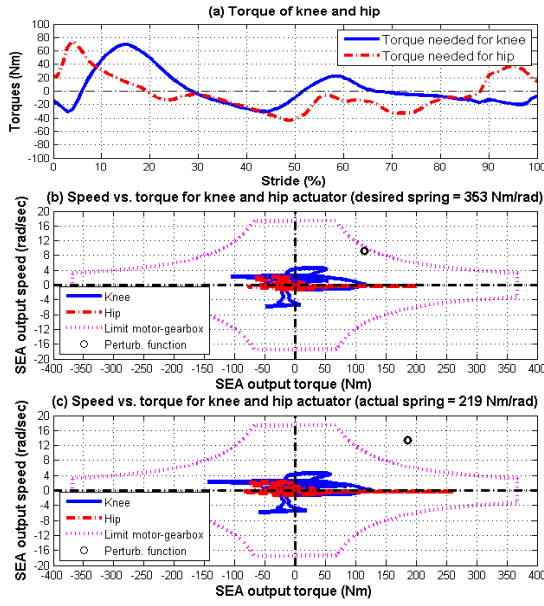
Fig. 2. (a): Torque needed to move the user's leg and exoskeleton frame. Torque-speed profile of the motor needed to provide full support with the desired spring stiffness of 353 Nm/rad (b), with the actual spring stiffness of 219 Nm/rad (c). The "Perturb. function" refers to the worst case scenario when switching from zero-impedance to maximal torque required during gait. The limitations of the chosen motor-gearbox combination are shown in (b) (c) as dotted pink lines.

The output of the actuator should have the option to be blocked at any joint position and should be able to resist 100 Nm. It should be possible to quantify the applied torque.

B. Design

1) Actuation

The authors have chosen to design an electric Series Elastic Actuated Joint (eSEAJ), directly mounted on the exoskeleton frame. For the drive system a brushless DC motor (Emoteq HS03801) has been chosen, as it is relatively lightweight and easy to incorporate into new designs. It is operated at 150 V and offers a peak torque of 10.5 Nm. Continuous power is 275 W and peak power is 1.68 kW.

For the gearbox a lightweight Harmonic Drive (CSG-20-50-2A-GR-E-SP) with a transmission ratio of 50 has been chosen, offering a good trade-off between maximal output torque and maximal gearbox input and output speed. The total weight of the motor-gearbox combination is 1107 g.

2) Elastic element

The design of the elastic element is of vital importance as it defines the maximal large torque bandwidth and force fidelity of the actuator [17]. In order to create a compact and rather stiff spring, it has been decided to rely on the double spring design (see Fig. 4) proposed by [18]. The spring is adapted to the needs of the new SEA. A maximal torque of 100 Nm is built up before the spring windings will block each other. Beyond 100 Nm the actuator output stiffness is rapidly increased. The double spiral design has the advantage to cancel out undesired radial forces acting on the spring centre when the spring is wrapping or unwrapping.

Design values	Goal	Achieved	Units
Peak torque	100	> 100	Nm
Actuator output speed	9.2	12.5	rad/s
Maximal mass	2	3.175	kg
Large torque bandwidth for 100 Nm, F_{LT}	5	6.9	Hz
Torque resolution	– [1]	< 0.05	Nm
Zero-impedance torque limit F_{ZIL} (Peak to peak)	0.5	/	Nm
Zero-impedance bandwidth, F_{ZI}	20	76	Hz
Spring stiffness, K_s	353	219	Nm/rad

In order to make the spring as lightweight and compact as possible maraging steel (AISI grade 18Ni, 350) has been chosen. It offers a yield tensile strength of 2320 MPa and has a modulus of elasticity of 200 GPa. The mass of the spring is 235 g with a thickness of 15 mm and a diameter of 75 mm.

The calculation of the spring design is based on simple beam bending equations which have been further refined by equations from [12]. The result of the calculation has been compared to FEA simulation results from ANSYS Workbench© and COSMOS Works©. For the calculation the applied torque has been divided by a factor of two, as the equations for the spring give only a result for one spring winding. This is thought to be legitimate as a double spiral spring should give the same result as two single spring windings acting in parallel.

3) Sensors

All required control information, i.e. spring deflection and joint rotation, can be measured with two position sensors. Two incremental encoders (Avago AEDA 3300), with a resolution of 80'000 pulses per revolution in quadrature decoding mode, are used. The theoretical output torque resolution is 0.0277 Nm. In addition a potentiometer (SAKAE FCP12AC) is used to measure the absolute position of the actuator output during the initialization procedure.

A torque sensor (2 strain gauge rosettes CFCA-3-350-23 from TML in a 90º configuration) has been added to the motor housing. The torque sensor gauges the torque during isometric measurements and serves as a safety to allow for intervention (e.g. break the motor) if the torque would exceed 100 Nm.

4) Control

The sensor signals are fed to the controller via two NI cards (NI PCI-6025E, NI PCI-6602). All cables connected to the NI cards are shielded, grounded and twisted. The NI cards are interfaced with a CPU. The system runs a Matlab© Kernel for xPC© target applications. The target computer communicates via Ethernet with a host computer where all data is processed.

For most tests a simple torque controller has been used to validate the eSEAJ characteristics. In some cases an impedance controller has been implemented.

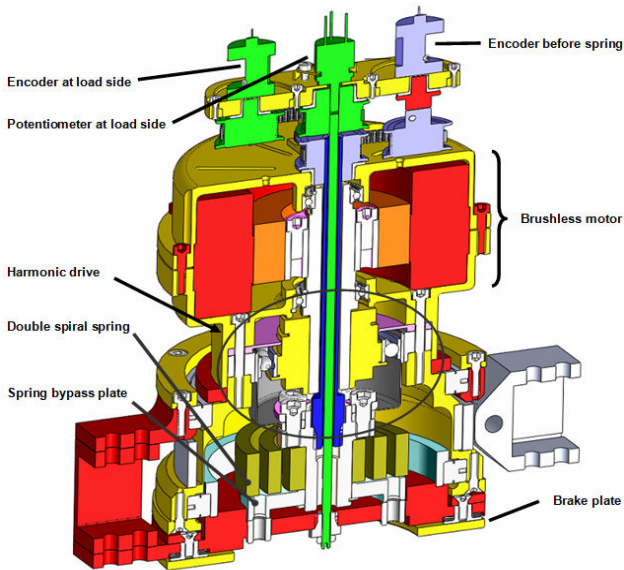The output signal of the controller is fed to an analogue

Fig. 3. Section view of the eSEAJ.

servo amplifier drive (AMC B40A20R) with trapezoidal commutation method. The actuator is powered with a DC power supply (Delta Elektronika SM 300-20).

5) Mechanical design

The overall mass and complexity of the exoskeleton is reduced, as the eSEAJ is a combination of a SEA and joint. The main parts, i.e. the brushless motor in series with the gearbox and the double spiral spring, are as compact as possible under the condition to be easily replaceable. All housing parts were made of aluminium 7075-T6. It has been decided to place the sensor part on top of the motor to facilitate replacement. For the sensor part, a potentiometer and one incremental encoder are connected to the actuator load side and one incremental encoder to the output of the gearbox. Two inner axles transfer the rotational motion from the rotating parts to the top of the actuator (see Fig. 3). The position sensors are connected via pre-tensioned tooth belts to the axles.

In order to increase fail-safety during tests, the actuator housing is thicker than necessary. The overall weight of the actuator is 3.175 kg. The actuator total height is 185 mm and the diameter is 109 mm.

The actuator output can be blocked with pins allowing isometric measurements at power-off. The spring can be bypassed and the SEA can behave like a conventional actuator. During tests the eSEAJ is mounted on a test bench. There are two ways to test the eSEAJ. First the actuator output is fixed

C. Validation

As the actuator is used for gait rehabilitation, different tests were executed. The performance of the motor is checked and the characteristics of the eSEAJ are validated only in a "static test configuration" test, where the actuator output is fixed (see Fig. 4).
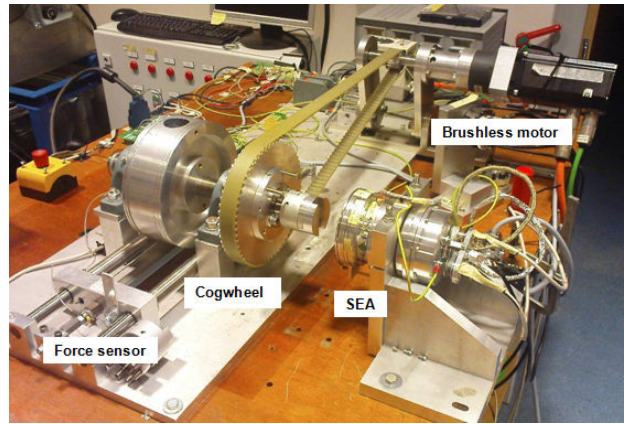

Fig. 4. The electric SEA joint on the test bench, enabling for different tests.

III. RESULTS

1) Actuation

The DC motor provides more than sufficient power for all scenarios. However, a back-driving torque of 8 Nm in cold state is determined. For small output torques, e.g. 5 Nm, the control bandwidth of the eSEAJ is 76 Hz using a 20 Nm (40 Nm peak to peak) multisine signal (using a flat amplitude spectrum in velocity domain). This control bandwidth limit is defined as a 3 dB drop. Defining the control bandwidth with a 90° phase lag, the limit would be 63 Hz. The multisine signal was repeated over 12 trials and the results have been averaged. The large torque bandwidth limit for 100 Nm output torque (200 Nm peak to peak) is 6.9 Hz, when reaching motor saturation. This result was achieved by generating sine sweep signals with different torque amplitudes ranging from 1 to 100 Nm (see Fig. 6). A spectral/-frequency analysis of each signal response was performed to generate a Bode plot. For the data points in Fig. 6 the large torque bandwidth values at -3 dB were used. The torque resolution is assessed to be at least 0.05 Nm.

2) Elastic Element

Under loading conditions the spring stiffness is nearly linear (see Fig. 7) until it reaches the point where the windings touch each other.
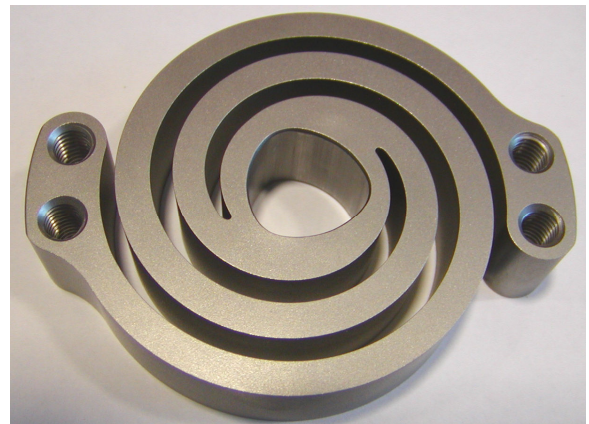

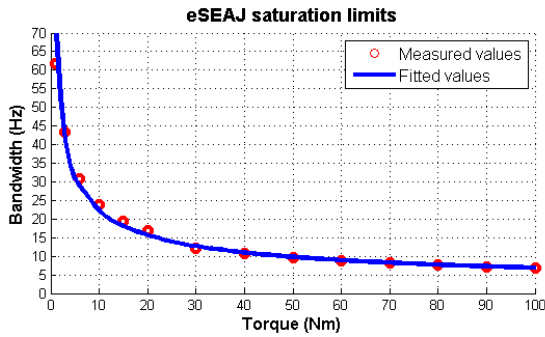Fig. 5. Double spiral spring. The inner bore shows a P3G-polygone profile.

Fig. 6. Plot of the large torque bandwidth limitation due to saturation of the actuator. At 100 Nm the bandwidth is 6.9 Hz. Values are fitted with cubic spline data interpolation (y = 71.792 x^-0.5093).

Fig. 7. Estimated spring stiffness: 219 Nm/rad. Notice the hysteresis.

The spring stiffness differs considerably from what has been calculated and simulated. The real spring stiffness is only 219 Nm/rad instead of the calculated and simulated 353 Nm/rad. Moreover, the windings start touching each other around 90 Nm instead of 100 Nm in each direction of rotation. During unloading hysteresis is observed.

3) Sensors

Signal noise is induced due to the magnetic field of the motor. In spite of this, the encoders give good results. The potentiometer resolution of 0.1 deg is sufficient to determine the absolute output position. The signal noise, induced during actuation, causes the potentiometer resolution to decrease to 3.92 deg. The strain gauge signal resolution of 18.22 Nm (RMS) is unacceptable.

4) Control

For the torque controller of the eSEAJ a simple PID controller with gain values KP=0.4, KI=5, KD=0.004 has been used. These values were identified with the Ziegler/Nichols method.

Step responses with different torque amplitudes have been generated to estimate stability. Steps in the range of 0.1 Nm to 1 Nm and 3 Nm to 60 Nm have been tested. It has been found that for small torques below 0.5 Nm the peak overshoot is larger than 20 %. Starting at 3 Nm the Peak overshoots are increasing from 10 to 20 % with increasing torque amplitude. The settling time is 0.35 seconds (measured when the overshoot drops below 1 %).

5) Mechanical design

The overall design is very robust as it can withstand torque peaks of 100 Nm without noticeable problems.

Unfortunately the spring broke during the trials when a sign error in the control scheme occurred, creating a torque beyond 200 Nm. Thus no data results are available for the "patient-in-charge" mode at zero impedance. Only an objective opinion by the authors during a manual trial can be given. No disturbing forces could be felt at the eSEAJ output in zero-impedance mode. Clearance between the gearbox shaft and the spring could be observed due to irregularities in the manufacture tolerances. As a result the control bandwidth decreases. The clearance has been eliminated by gluing both parts together.
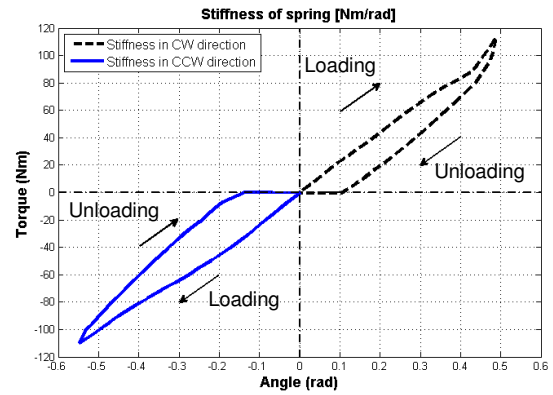
The mechanical configuration of the sensor part is reliable and no clearance could be observed. However, it has been found that excessive pretension of the belts causes the inner axles to deform. This evokes forces which damage the potentiometer's bearing.

The mechanism to block the actuator output, which is based on friction, could only withstand a torque of 53 Nm.

IV. DISCUSSION

1) Actuation

The actuator is backdrivable in every state but needs a breakaway torque of 8 Nm. This is due internal friction in the Harmonic Drive. In case of abrupt power supply failure this could be advantageous as the user motion is damped. Alternatively the Harmonic Drive could be replaced by a more efficient planetary gearbox.

The control bandwidth of 76 Hz (or 63 Hz) and the large torque bandwidth of 6.9 Hz are excellent results. A large torque bandwidth of 6.9 Hz at 100 Nm is more than sufficient and the "robot-in-charge" mode can provide sufficient torque at different speeds. It should be remembered that the spring stiffness is only 2/3 of the calculated stiffness. Thus the motor needs to provide more power to reach 100 Nm. With a spring stiffness of 353 Nm/rad, a weaker and more lightweight motor could be used.

2) Elastic element

High output torque resolution results from the combination of incremental encoders and an elastic element. As expected the spring stiffness is quite linear until the windings start touching each other.

The hysteresis effects cannot be explained. They might be due to compliance in the test setup. Some of the spring stiffness difference can be explained by a missing heat treatment during the manufacture procedure and by differences of the simulated and the real spring behaviour. The calculations and simulations of the von Mises stress and the spring stiffness need to be revised. The chosen ductile material allows for acceptable behaviour during repeated deformation, even though the spring broke at overload. For future designs it is crucial to find out how

the stiffness of the spring design could be reliably predicted. For now no explanation can be given. More tests and more simulations should be performed in order to find a relation between theory and reality.

3) Sensors

The sensors are influenced by the electromagnetic field of the motor. The potentiometer signal is not useful when the motor is running. At power off the potentiometer can be used as an absolute position sensor. In order to prevent problems in future designs the sensors could be integrated inside the actuator housing, which would also make all sensor axles and the tooth belt system dispensable.

4) Control

Due to spring failure further testing had to be abandoned but is recommended for future work. The torque controller (PID) is close to its optimal values. From a Nyquist plot of the open-loop gain of the torque controller it could be identified that the closed loop system will have an overshoot of 10%. This is an acceptable value.

The large step response overshoot for small torques is due to limitations in sensor resolution. For larger torques, the overshoot increase is caused by rotational inertia in the actuator. The settling time is acceptable as well.

5) Mechanical design

Signal noise has been induced on the sensor part as the aluminium housing is unable to shield the magnetic field. A steel motor housing could prevent the induction of voltages in the sensor part, but will increase overall weight. The bending of the axles, which increases the wear of the sensors' bearings, is caused by the one-sided suspension of the pulleys and the encoders. A double-sided suspension would solve this problem, but increase complexity and weight of the sensor part. Alternatively the arrangement of the sensors could be changed, as already proposed.

An overall mass of 2 kg could be achieved by decreasing the overall wall thickness of the housing parts and using a more lightweight motor. The motor output friction brake is not effective and requires redesign.

V. CONCLUSION

The mechanical design is robust and can withstand an output torque of at least 100 Nm. The spring stiffness is quite linear. The actuator bandwidth is sufficient and meets the requirements. The design can be improved by decreasing the overall mass to 2 kg.

For future designs the spring simulation procedure should be checked and the sensor positions should be revised. Regarding all these aspects it can be concluded that this newly developed actuator is a feasible alternative to actuate the joints in LOPES.

REFERENCES

[1] American Heart Association. International cardiovascular disease statistics. [Online], 2007. Statistical Fact Sheet — Populations 2007 Update.

[2] American Heart Association. Heart disease and stroke statistics - 2009 update (at-a-glance version). [Online], 2009. Heart Disease and Stroke Statistics — 2009 Update.

[3] S. K. Au, P. Dilworth, and H. M. Herr. An ankle-foot emulation system for the study of human walking biomechanics. *Robotics and Automation, 2006. ICRA 2006, Proceedings 2006 IEEE International Conference on*, pages 2939–2945, May 2006.

[4] L. L. Cai, A. J. Fong, C. K. Otoshi, Y. Liang, J. W. Burdick, R. R. Roy, and V. R. Edgerton. Implications of assist-as-needed robotic step training after a complete spinal cord injury on intrinsic strategies of motor learning. *Journal of Neuroscience*, 26(41):10564–10568, Oct 2006.

[5] Dined. Anthropometric data. [Online] www.dined.nl , 2004.

[6] J. L. Emken, J. E. Bobrow, and D. J. Reinkensmeyer. Robotic movement training as an optimization problem: designing a controller that assists only as needed. *Rehabilitation Robotics, 2005, ICORR 2005. 9th International Conference on*, pages 307–312, Jun -1 Jul 2005.

[7] N. Hogan. Impedance control: An approach to manipulation: Part i - theory, part ii - implementation, part iii - applications. *Journal of Dynamic Systems, Measurement and Control*, pages 1–24, 1985.

[8] N. Hogan. Stable execution of contact tasks using impedance control. *Robotics and Automation. Proceedings, 1987 IEEE International Conference on*, 4:1047–1054, Mar 1987.

[9] G. Kwakkel, B. J. Kollen, and H. I. Krebs. Effects of robot-assisted therapy on upper limb recovery after stroke: a systematic review. *Neurorehabil Neural Repair*, 22(2):111–121, Sep 2008.

[10] F. Levi, F. Lucchini, E. Negri, and C. La Vecchia. Trends in mortality from cardiovascular and cerebrovascular diseases in europe and other areas of the world. *Heart*, 88(2):119–124, Aug 2002.

[11] M. Lotze, C. Braun, N. Birbaumer, S. Anders, and L. G. Cohen. Motor learning elicited by voluntary drive. *Brain*, 126(Pt 4):866–872, Apr 2003.

[12] W. Matek. *Roloff/Matek Maschinenelemente: Normung, Berechnung, Gestaltung*, pages 277–278. Vieweg & Sohn Verlag, Braunschweig/Wiesbaden, 9 edition, 1985.

[13] G. B. Prange, M. J. A. Jannink, C. G. M. Groothuis-Oudshoorn, H. J. Hermens, and M. J. Ijzerman. Systematic review of the effect of robot-aided therapy on recovery of the hemiparetic arm after stroke. *J Rehabil Res Dev*, 43(2):171–184, Mar/Apr 2006.

[14] J. E. Pratt, B. Krupp, and C. Morse. Series elastic actuators for high fidelity force control. *Industrial Robot: An international robot*, 29(3):234–241, 2002.

[15] D. J. Reinkensmeyer, D. Aoyagi, J. L. Emken, J. A. Galvez, W. Ichinose, G. Kerdanyan, S. Maneekobkunwong, K. Minakata, J. A. Nessler, R. Weber, R. R. Roy, R. de Leon, J. E. Bobrow, S. J. Harkema, and V. R. Edgerton. Tools for understanding and optimizing robotic gait training. *J Rehabil Res Dev*, 43(5):657–670, Aug/Sep 2006.

[16] D. W. Robinson and G. A. Pratt. Force controllable hydro-elastic actuator. *Robotics and Automation, 2000. Proceedings, ICRA '00 IEEE International Conference on*, 2:1321–1327, Apr 2000.

[17] A. H. A. Stienen. *Development of novel devices for upper-extremity rehabilitation*. PhD thesis, University of Twente, Twente, The Netherlands, Jan 2009.

[18] A. H. A. Stienen, E. E. G. Hekman, H. ter Braak, A. M. M. Aalsma, F. C. T. van der Helm, and H. van der Kooij. Design of a rotational hydro-elastic actuator for an active upper-extremity rehabilitation exoskeleton. pages 881–888, Oct 2008.

[19] J. F. Veneman, R. Kruidhof, E. E. G. Hekman, R. Ekkelenkamp, E. H. F. van Asseldonk, and H. van der Kooij. Design and evaluation of the lopes exoskeleton robot for interactive gait rehabilitation. *Neural Systems and Rehabilitation Engineering, IEEE Transactions on*, 15(3):379–386, Sep 2007.

[20] D. A. Winter. *Biomechanics and Motor Control of Human Movement*. John Wiley & Sons, Inc, 4th edition, 1990.